Développement d'un système de mesure ultrasonore à base de réseaux de Bragg sur fibre optique : application au contrôle santé intégré par ondes élastiques guidées

Arnaud Recoquillay, Nicolas Roussel, Laurent Maurin, Tom Druet, Guillaume Laffont, Bastien Chapuis

Development of an ultrasonic wave measurement device based on Fiber Bragg Gratings in optical fibers: application to Guided Wave Structural Health Monitoring

Arnaud Recoquillay[1*], Nicolas Roussel[1], Laurent Maurin[1], Tom Druet[1], Guillaume Laffont[1], and Bastien Chapuis[1]

[1] Université Paris-Saclay, CEA, List, F-91120, Palaiseau, France

*corresponding author, E-mail: arnaud.recoquillay@cea.fr

Abstract

Optical fiber transducers such as Fiber Bragg Gratings (FBG) are promising solutions for guided waves Structural Health Monitoring (SHM) due to their low intrusivity and their ability to cope with harsh environments (extreme temperatures, radiations, explosive atmospheres…). We present here a solution enabling measurements under varying environmental and operational conditions, which is mandatory for many applications in SHM, the low complexity of the solution ensuring good integration capacities. The effect of the length of the FBG was also studied to enable the optimization of the system sensitivity.

1. Introduction

Ultrasonic guided waves have been studied for nondestructive testing applications for a long time [1] and, more recently, also for Structural Health Monitoring (SHM) [2]. Indeed, these waves propagate over large distances in waveguides such as plates, pipes or rails, making them suited for many applications and enabling to inspect a large portion of a structure with only a few sensors. In particular, for SHM, this helps limiting the intrusivity of the system. However, conventional sensors, which use piezoelectric transducers, may not be suited: they may add too much weight, need lots of circuitry and cannot withstand harsh environments in general. On the other hand, optical fiber sensors have been used in many applications due to their low intrusivity and ability to cope with harsh environments such as extreme temperatures, electromagnetic environments, or radiations. They have been used in many low frequency applications, based for instance on distributed [3] and accurately localized measurements [4]. However, such distributed measurements, also like Distributed Acoustic Sensing [5], are rather limited in terms of sampling frequency and spatial resolution, making their use for ultrasonic measurements inadequate as of today. Hence the use of quasi-distributed optical fibers transducers for ultrasonic measurements, such as Fiber Bragg Gratings, is one solution. To achieve the high sampling frequency necessary for these measurements, most solutions are based on the so-called « edge filtering » technique [6][7] briefly described hereafter. Contrary to piezoelectric transducers, FBG transducers are not able to emit ultrasonic waves. That is why they have been recently used for passive acquisitions [8], that is the recovery of equivalent signals to classic inspections with emitters from the acquisition of ambient noise in the structure. This has been later combined to guided wave imaging [9]. A SHM system can hence be designed using solely these transducers, reducing greatly the system's intrusivity thanks to the small diameter of the optical fiber, enabling perfect integration properties, especially in composite structures [10], combined with the multiplexing capabilities in a single optical fiber.

However, FBG acquisition systems are sensitive to variations in Environmental & Operational Conditions (EOC), as the FBG itself is sensitive to strain & temperature changes. Previous studies have proposed optoelectronic systems correcting this sensitivity, but needing additional assumptions such as two FBGs submitted to the same EOCs [11] or the same ultrasonic waves [12], or with a rather high complexity which may hinder their integration capabilities [13]. We propose here a solution close to [14], enabling to filter out low frequency EOC variations from the measurements. This solution is based on the real-time tracking of the setting point of the edge filtering technique thanks to a thermal tuning of the laser source. This solution was tested during a four points bending test of a flat composite sample. The sensitivity of the edge filtering technique was also studied experimentally to determine the length of the Fiber Bragg Grating with respect to the ultrasonic wavelength of interest. The system and its validation are presented in the next section, while the optimization of the FBG length is the subject of the third section.

2. Ultrasonic measurements using Fiber Bragg Gratings under dynamic environmental conditions

Fiber Bragg Gratings are the result of local variations of the refractive index of the core a singlemode optical fiber, leading to the reflection of light in a narrow band, around a center wavelength, the so-called Bragg wavelength λ_B. More precisely, for the simplest FBGs, *i.e.*: with periodic variations of this refractive index, λ_B is given by:

$$\lambda_B = 2n_{eff}\Lambda \quad (1)$$

where n_{eff} is the effective refractive index of the waveguide, and Λ is the grating pitch. To adapt the reflected spectrum with respect to an application, different kinds of gratings can be considered. For example, to limit sidelobes in the spectrum, apodized FBGs can be used [15]. The ultrasonic measurement principle can easily be understood from (1): an incident wave will induce a change in the grating pitch Λ, leading to a shift $\delta\lambda_B$ in the Bragg wavelength. Theoretically, the real-time measurement of λ_B, based for instance on a peak detection algorithm, could be used to detect the incident wave. But the strain variation induced by the Lamb waves (typically lower than 0.1 µm/m) is at least one order of magnitude lower than what can be achieved with such method for today's monitoring systems, mainly dedicated to strain and temperature metrology, with measurement rates still not compliant with ultrasonic (> 10 kHz) frequencies. Moreover, depending on the ratio between the FBG length and the ultrasonic wavelength, the effect of the incident wave on the reflected spectrum may be more complex than a simple translation [16]. Hence the use of another technique, named *edge filtering*, is mandatory.

2.1. Edge filtering

The principle of edge filtering is depicted in Figure 1.

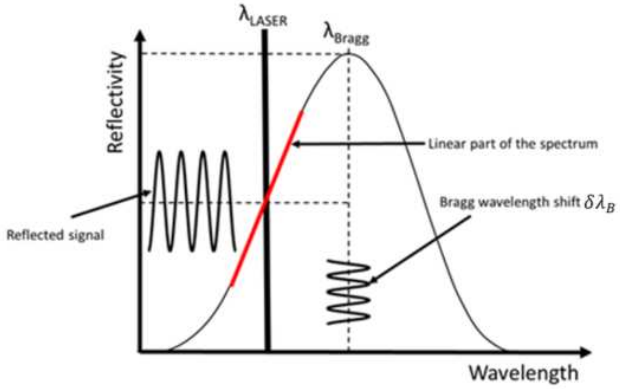

Figure 1: Principle of edge filtering

As mentioned, the reflected spectrum of a FBG is characterized by a narrow band peak. It is however possible to lock a narrower light source, such as a laser, on one edge of this peak, and in particular around its half maximum. The light source must be of constant power, so that if the edge of the peak shifts, the reflected power varies proportionally, the spectrum being quite linear around its half maximum. Note that this shift occurs independently of the ultrasonic wavelength [16]. It then suffices to use a photodiode to convert the light into a voltage, which can then be amplified, filtered and lastly digitized using an Analog to Digital Converter (ADC), for further analysis.

2.2. Setting point tracking

The principle of edge filtering was successfully used in many laboratory applications until now. However, as mentioned in the introduction, FBGs are also sensitive to many EOCs such as temperature or strain changes. More specifically, the changes of the Bragg wavelength are given by the Bragg relationship [17]

$$\frac{d\lambda_B}{\lambda_B} = (\kappa_T + \kappa_\varepsilon \Delta\alpha)dT + \kappa_\varepsilon d\varepsilon_{struct} \quad (2)$$

where κ_T and κ_ε are respectively the sensitivity to temperature and longitudinal strain of the FBG, $\Delta\alpha$ is the difference in thermal expansion coefficients between the optical fiber and the host structure, and $d\varepsilon_{struct}$ is the mechanical strain variation component of the structure in the direction of the FBG transducer.

From (2), variations in EOCs lead to a wavelength shift in the position of the peak, resulting in a loss of sensitivity of the system as the peak drifts away from the laser wavelength, up to a null sensitivity for important EOC changes if the laser wavelength, supposed to be locked on one edge of the FBG spectrum, is not corrected.

The variations in EOCs are supposed to occur at lower frequencies than the ultrasonic frequencies. As can be seen in section 2.1, in edge filtering, ultrasonic waves are measured through small oscillations of the output voltage around a constant value, which is directly linked to the setting point, that is the relative position of the laser wavelength to the FBG wavelength. This setting point can hence be tracked through the control of the DC output of the photodiode.

More precisely, a DFB laser source is used in this application: its emitting wavelength can be tuned through a thermal effect with a Peltier device controlled by a PI control loop on the DC component, the multiplicative coefficient being corrected to take into account the nonlinear response of the DFB laser source to temperature. To avoid unnecessary corrections, it was also decided to divide the DC value range into three areas: a first area around the nominal value, in which no tuning is performed, and two areas, above and below this nominal area, in which the PI control loop applies a correction, so that the DC value if forced to go back into the nominal range. The sensitivity to ultrasonic waves remains indeed the same for all values in the first range.

2.3. Experimental validation

The setup was tested during a 4-points bending test. The two bottom external supports are 22 cm apart while the two top internal supports are 16 cm apart. A Fiber Bragg Grating was glued at the center, on the bottom surface of a flat composite sample. The 4 mm long type-III FBG (femto-second photo-writing process) is apodized to avoid side lobes. During the test, the maximum vertical displacement of the two center points was set at 32 mm, leading to a Bragg wavelength shift slightly smaller than 1 nm. The displacement speed varied between 0.5 mm/min and 7 mm/min, with a 0.5 mm/min increase between each step. By doing so, the capacity of the system to stay tuned under increasing strain rates could be tested. A 10 mm diameter piezoelectric transducer was coupled using shear gel at one end of the plate to act as an actuator. It is actuated using a low frequency generator, which emits a 5 cycles Hann burst

of center frequency 40 kHz and amplitude 10 Vpp, with a burst period of 100 ms to enable several acquisitions during the bending test. An analog first order band-pass filter between 10 kHz and 300 kHz is also used in reception to limit noise outside the ultrasonic frequencies. A reference FBG, on another optical fiber, was also glued alongside the first FBG, to get an image of the sample deformation.
The optoelectronic system was set so that the maximum output voltage of the photodiode was 10 V, inducing an optimum setting point at 5 V. The area without tuning is set empirically between 4 V and 6 V. During the experiment, the DC voltage is acquired as our tuning parameter. The wavelength of the reference FBG is measured using a Micron-Optics™ Si255 monitoring system. The corresponding data are plotted in Figure 2.

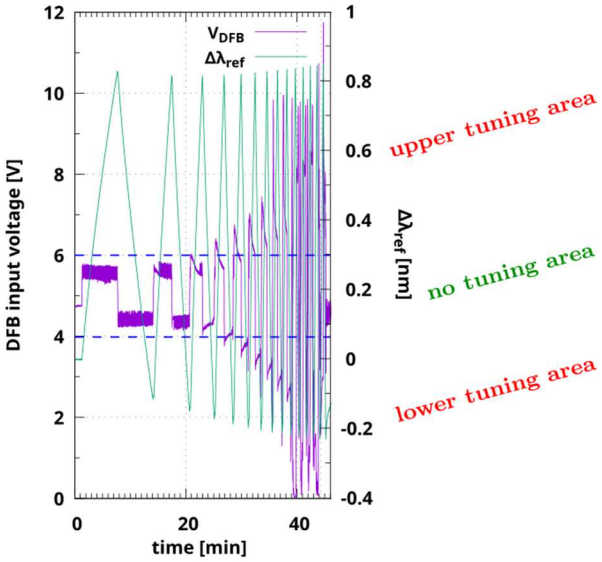

Figure 2: Evolution during the four points bending test of the DFB laser diode control DC input voltage $\boldsymbol{V_{DFB}}$ and the wavelength shift $\boldsymbol{\Delta\lambda_{ref}}$ of a control FBG transducer glued on the flat composite sample.

In this figure, the control FBG gives an image of the endured deformation by the flat sample at increasing speeds, its variations being in the prescribed range. We can see that the DC voltage remains between the prescribed boundaries for the first steps, with small corrections occurring continuously to adjust in real-time the DFB laser wavelength. As the speed increases, an overshoot appears as the solicitation direction changes: as our system is based on a thermal effect, it presents some inertia, leading to the system still shifting the laser source in a direction while the solicitation already goes in the opposite. Note however that this overshoot is mainly due to the selected solicitation shape, and may not be representative of field applications. The system is then able to go back into the "no tuning area". For fastest solicitations, the system is not able anymore to compensate, resulting in a DC voltage that remains most of the time within the tuning areas.
From this test, we estimated that the tracking has been performed without any sensitivity degradation up to a strain rate of 17 (µm/m)/s for the sample under test. For higher strain rates, there will first be a loss of sensitivity when the setting point is still on either side of the reflection spectrum, that is for DC voltages above 2 V and below 8 V empirically. Then, for even higher strain rates, the setting point may be lost and the system will then seek for the FBG spectrum, leading to a temporary blind zone. In this specific test, this blind zone lasted at most a few seconds. The corresponding strain rates could not be estimated as the step was too short given the time corresponding to the overshoot. Ultrasonic signals were also acquired to assess the good quality of the data at four different times during the test. Examples of such signals are plotted in Figure 3.

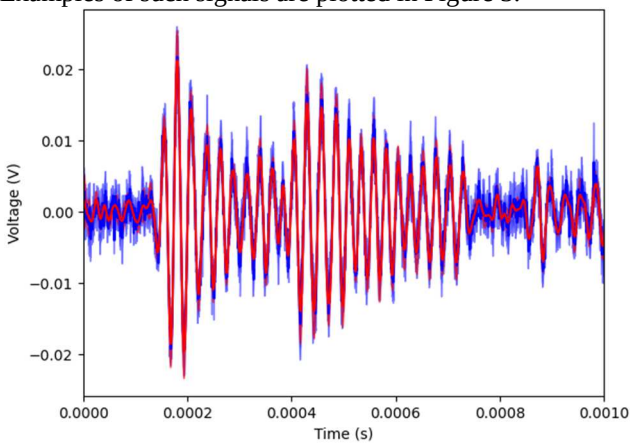

Figure 3: Acquired ultrasonic signals during the four points bending test. Lines correspond to the mean signal over different acquisitions, shaded areas correspond to 3 standard deviations around the mean value. Blue: raw signal. Red: band-pass filtered signal.

In this figure, the lines correspond to the mean signals, the mean being taken over the different acquisition times, one of them being acquired in static conditions as a reference. The shaded areas around the curves correspond to a 3 standard deviation around the mean value. Raw data are plotted in blue, and numerically filtered data around the center frequency are plotted in red. Note that in this figure and for the remaining of the section, the data are not normalized, so that the amplitudes can be compared between figures. Only small variations around the mean value are observed, with a good signal to noise ratio even for the raw data. We then computed the residual signals between each acquisition and the reference one, acquired in static conditions. The corresponding signals are plotted in Figure 4.

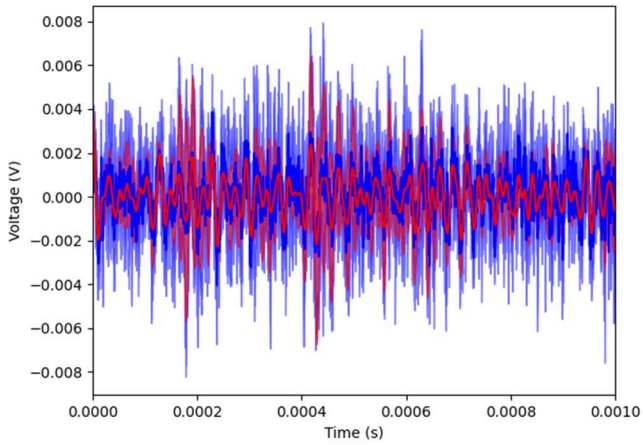

Figure 4: Residual signals using the data acquired in the static case as a reference. Lines correspond to the mean signal over different acquisitions, shaded areas correspond to 3 standard deviations around the mean value. Blue: raw signal. Red: band-pass filtered signal.

The order of magnitude of the residuals is close to 10% of the magnitude of the original signals, with no clear evolution versus time: these residuals might result mainly from measurement noise. To get confirmation, we also acquired averaged data over 10 consecutive samples. The quantity of samples was kept low to avoid any averaging effect over the evolution of the deformation, the change of geometry and strain rate of the host structure, which may indeed have an effect on the guided wave signal. The residual signals obtained from the averaged data are plotted in Figure 5.

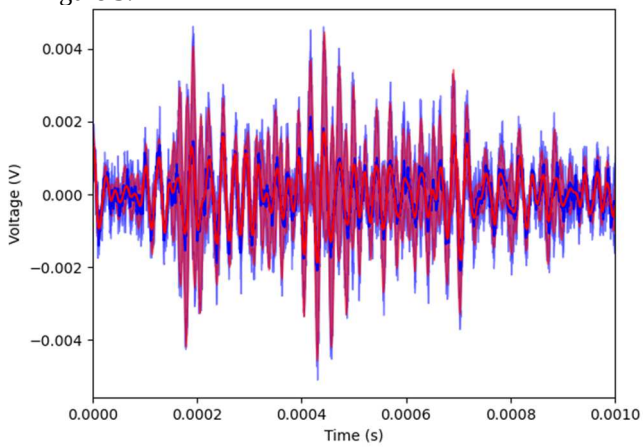

Figure 5: Residual average signals using the data acquired in the static case as a reference averaging each acquisition over 10 consecutive samples. Lines correspond to the mean signal over different acquisitions, shaded areas correspond to 3 standard deviations around the mean value. Blue: raw signal. Red: band-pass filtered signal.

The amplitude of these residuals has further decreased due to the averaging, confirming that a significant part of these residuals is due to measurement noise.

3. Bragg length optimization

The previous section shows ultrasonic waves measurements using FBGs under dynamic loading with a satisfactory signal to noise ratio. However, no specific attention was paid on the choice of the FBG. This choice may be significant to improve the sensitivity of a system. Furthermore, as several guided modes may exist in a host structure at the frequency of interest, the choice of the transducer may help selecting the desired mode.

This question has been the subject of some studies in the past [16]. Broad qualitative behavior have been observed, in particular based on simulations [18]: in the first region, the FBG length is large with respect to the ultrasonic wavelength, leading to an averaging and no sensitivity. In the second region, where the FBG length is of the same order as the ultrasonic wavelength, the FBG peak is not only shifted but rather changes width due to the interaction with the incident wave. In the last region, in which the FBG length is small with respect to the ultrasonic wavelength, the FBG sees a uniform deformation field, leading to a quite homogeneous peak shift.

Experimental tests were performed in the second and third region [16], up to a Bragg length of half the ultrasonic wavelength but, to the author's knowledge, no study tried experimentally to use a FBG transducer in the first region, that is longer than the ultrasonic wavelength. The experiment presented hereafter aims at validating the FBG sensitivity with respect to the ultrasonic wavelength.

3.1. Experimental setup

The experimental setup is depicted in Figure 6: our aim is to acquire guided waves corresponding to different wavelengths using different lengths of FBGs, and to compare the corresponding amplitudes. To do so, a square aluminum plate of thickness 3 mm *vs.* 1 m side was used for the experiment to have a good knowledge of the ultrasonic guided wave wavelengths. A piezoelectric transducer was glued to the surface, and FBG transducers of different lengths, *i.e.*: 7 mm, 14 mm, 21 mm and 28 mm, were glued to the panel along a circle 200 mm apart from the emitter. This distance was chosen to have a good time separation over a large frequency range of the S0 and A0 modes without interference with modes reflected from the edges of the plate.

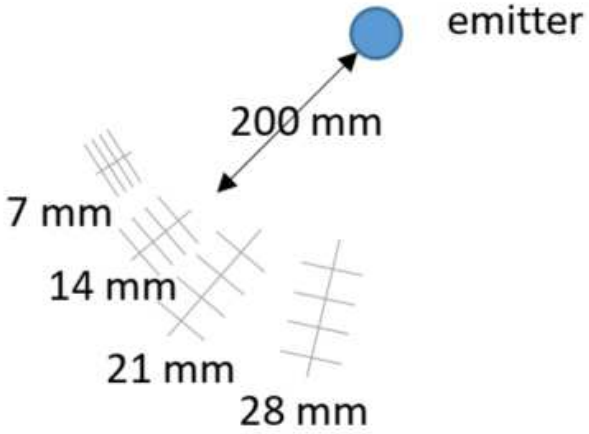

Figure 6: Scheme of the FBG transducers lengths optimization experiment.

The piezoelectric transducer was excited using a 5 cycles Hann burst with a center frequency varying between 20 kHz and 200 kHz, with a 20 kHz step. As it is well known that the excitation depends also on the shape of the emitter, data were acquired with piezoelectric transducers of different diameters, *i.e.*: 10 mm, 14 mm and 20 mm.
The data were acquired with the same kind of setup as in the previous section, but without any tracking of the setting point, the EOCs being stable. The data were also averaged over 100 samples to determine precisely the amplitude of the incident modes. Finally, these amplitudes were extracted through the maximum of envelope in a time window of 5 cycles around the theoretical time of flights. Examples of acquired signals with the position of the extracted maximum are plotted in Figure 7.
Finally, reference measurements were also performed using a laser interferometer at a normal incidence, also at 200 mm away from the source. This sensor is assumed to have a constant response with respect to frequency over the used range, enabling to compensate for the dependency of the emission. However, as it is only sensitive to the normal displacement at the surface of the sample, only values for the A0 mode could be retrieved. We hence focus on this mode in the next section. Note that, for the frequency range of our experiment, the A0 mode wavelength ranges between 7 mm and 38 mm, enabling to study the various sensitivity area mentioned before.

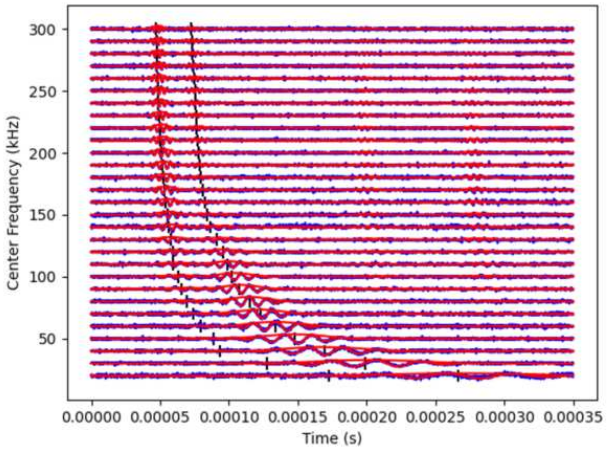

Figure 7: Acquired signals for a FBG length of 7 mm and an emitter of diameter 14 mm. Black lines indicate the extracted maximum of amplitude of S0 (first line) and A0 (second line). Blue: raw signals. Red: mean signals.

3.2. Results

First, the normalized extracted amplitudes are plotted with respect to frequency in Figure 8. In this case, the main factor is the emitter, as all curves corresponding to a given source show similar results.

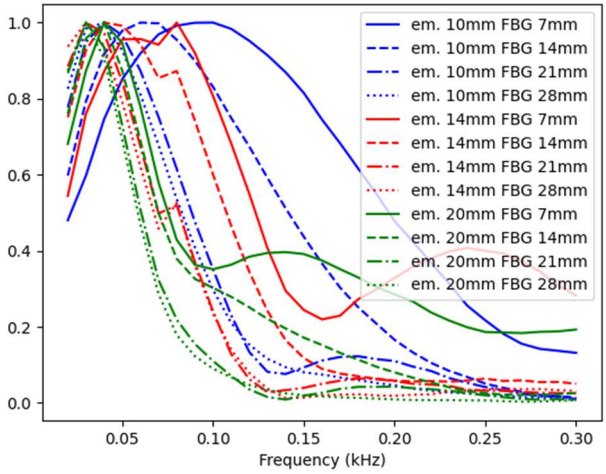

Figure 8: Normalized amplitude of A0 with respect to frequency for different emitter and receiver sizes, each curve being normalized with respect to its maximum value.

The same curves are then plotted with respect to the ratio between the FBG length and the ultrasonic wavelength in Figure 9. The data were also normalized with respect to the maximum measured amplitude for a given emitter, to reduce the effect of this parameter.

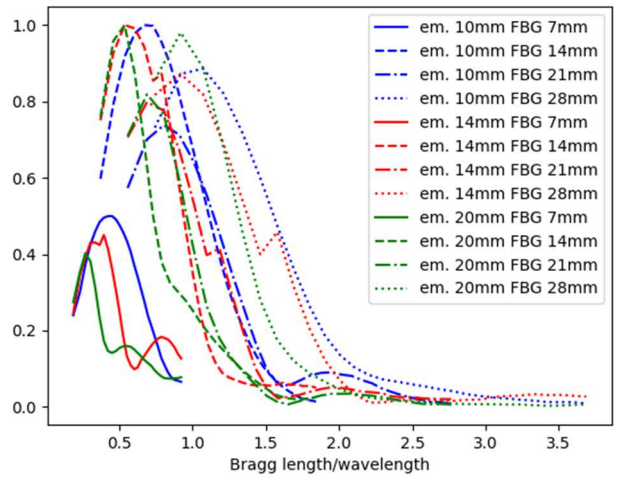

Figure 9: Normalized amplitude of A0 with respect to the ratio between FBG length and ultrasonic wavelength for different emitter and receiver sizes. The curves are normalized with respect to the maximum value for a given emitter.

We see that the maximum amplitude, independently of the emitter, is obtained for a ratio above 0.5, which tends to demonstrate that a longer FBG should indeed be used. Note however that the maximum sensitivity is always obtained for the FBG of length 14 mm, which also demonstrates that a too long FBG may result in a decrease in sensitivity, as expected. These effects on sensitivity for the edge filtering technique can be explained by two reasons: first, as mentioned before, a too long FBG results in an averaging effect along its entire length, limiting its sensitivity due to a reduced wavelength shift $\delta\lambda_B$ on the edges. But a longer FBG also means a narrower reflection peak, and so a steeper edge with a greater sensitivity. The best sensitivity compromise is then shifted towards longer FBGs.
It is however hard from this plot to deduce the best ratio, as the trends are still dependent on the emission.
Finally, the acquired data were normalized with respect to the amplitude acquired using the laser interferometer. The corresponding amplitudes are plotted in Figure 10.

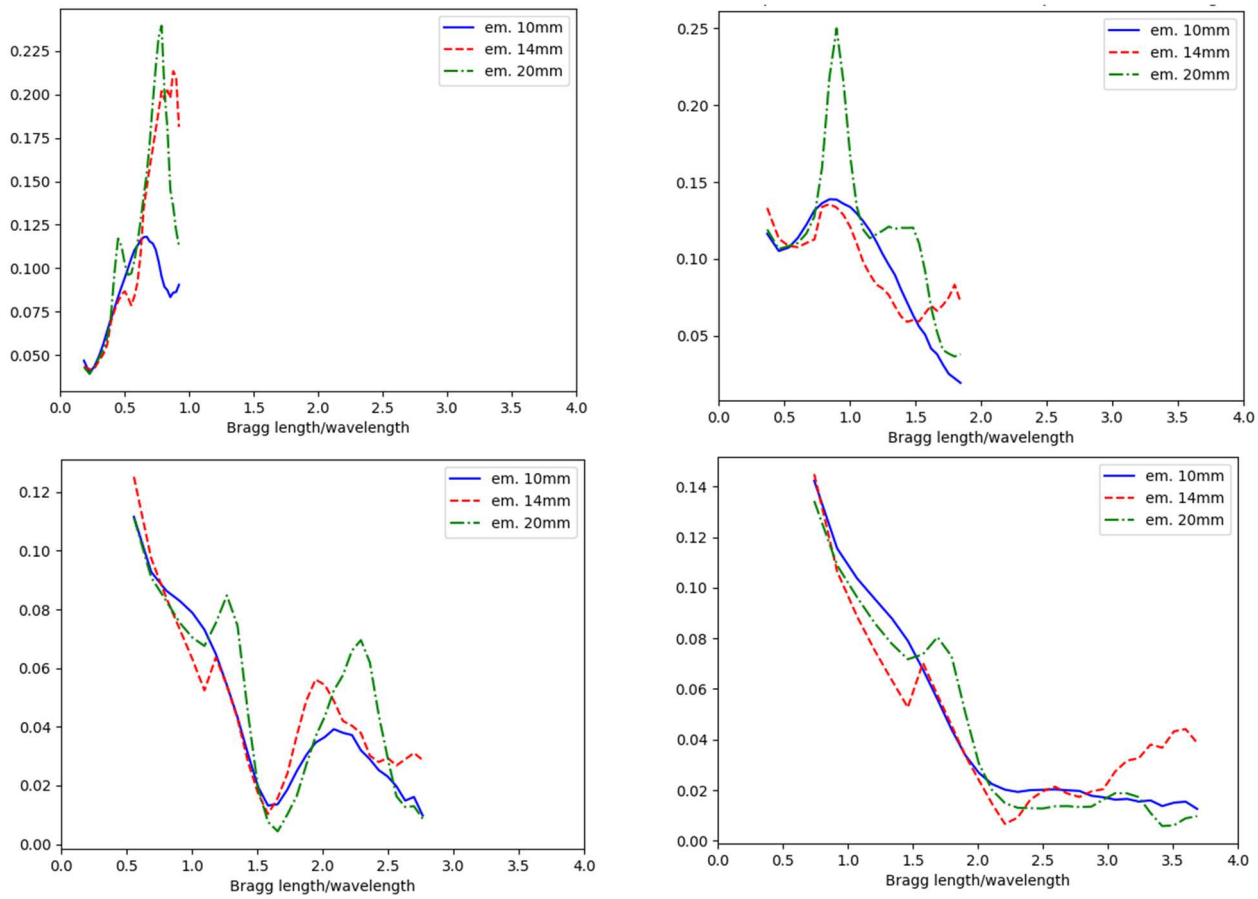

Figure 10: A0 amplitude normalized with respect to the measured emission amplitude using a laser interferometer. From left to right and top to bottom: FBG length of 7 mm, 14 mm, 21 mm and 28 mm.

First, we see a good agreement between the curves corresponding to different emitters in this case, showing that the effect of the emission has been properly compensated. Second, we see that a maximum is indeed obtained for a ratio between 0.5 and 1 in all cases, this maximum being around a ratio of 0.8. Note that the first points of all curves are polluted by interactions between S0 and A0 modes: indeed, for such a low frequency (20 kHz),

S0 has a too big wavelength to be separated. These points were left for the sake of completeness, but this interaction explains the local maxima at the first points, incoherent with the subsequent trends.
Finally, remark that FBG transducers are rather broadband sensors, as the sensitivity does not decrease too fast around the optimal value, making them good candidates for applications such as acoustic emission.

4. Conclusions

We have shown in this paper the possibility to use FBG transducers for ultrasonic wave measurements under varying Environmental & Operational Conditions. The proposed setup leads to a good signal to noise ratio with a rather simple setup, making it a good candidate for integration in a structural health monitoring system. The next step will be to use such a setup with several transducers multiplexed along the same optical fiber.
The sensitivity of the FBGs with respect to the ultrasonic wavelength was also studied, enabling to determine that the maximum sensitivity is indeed for a ratio between FBG length and ultrasonic wavelength around 0.8, which is a higher value than what has been studied in the past. It also appeared that their response is not varying strongly with the wavelength, and so the frequency, making them versatile sensors.

References

[1] Lowe, Mike JS, Alleyne, David N., and Cawley, Peter. "Defect detection in pipes using guided waves." *Ultrasonics* Vol. 36 no 1-5 (1998): pp. 147-154.

[2] Mesnil, Olivier, Recoquillay, Arnaud, Fisher, Clément, *et al.* "Self-referenced robust guided wave based defect detection: Application to woven composite parts of complex shape." *Mechanical Systems and Signal Processing* Vol. 188 (2023), pp. 109948.

[3] Ferdinand, Pierre, Magne, Sylvain, and Laffont, Guillaume. "Optical fiber sensors to improve the safety of nuclear power plants." In : *Fourth Asia Pacific Optical Sensors Conference*. SPIE (2013). pp. 359-362.

[4] Maurin, Laurent, Ferdinand, Pierre, Nony, Fabien, *et al.* « OFDR distributed strain measurements for SHM of hydrostatic stressed structures: an application to high pressure hydrogen storage type IV composite vessels-H2E project." In: *EWSHM-7th European Workshop on Structural Health Monitoring*.Nantes (2014).

[5] He, Zuyuan and Liu, Qingwen. "Optical fiber distributed acoustic sensors: A review." *Journal of Lightwave Technology*, Vol. 39 no 12 (2021), p. 3671-3686.

[6] Betz, Daniel C., Thursby, Graham, Culshaw, Brian, *et al.* "Acousto-ultrasonic sensing using fiber Bragg gratings." *Smart Materials and Structures* Vol. 12 no 1 (2003), pp. 122.

[7] Takeda, Nobuo, Okabe, Yoji, Kuwahara, Junichiro, *et al.* "Development of smart composite structures with small-diameter fiber Bragg grating sensors for damage detection: Quantitative evaluation of delamination length in CFRP laminates using Lamb wave sensing." *Composites science and technology* Vol. 65 no 15-16 (2005), pp. 2575-2587.

[8] Druet, Tom, Chapuis, Bastien, Jules, Manfred, *et al.* "Passive guided waves measurements using fiber Bragg gratings sensors." *The Journal of the Acoustical Society of America* Vol. 144 no 3 (2018), pp. 1198-1202.

[9] Recoquillay, Arnaud, Druet, Tom, Nehr, Simon, *et al.* "Guided wave imaging of composite plates using passive acquisitions by fiber Bragg gratings." *The Journal of the Acoustical Society of America* Vol. 147 no 5 (2020), pp. 3565-3574.

[10] Sansonetti, P. *et al.* "Intelligent composites containing measuring fiber-optic networks for continuous self-diagnosis". 198–209 (1991). doi:10.1117/12.50179

[11] Wu, Qi and Okabe, Yoji. "Investigation of an integrated fiber laser sensor system in ultrasonic structural health monitoring." *Smart Materials and Structures* Vol. 25 no 3 (2016), pp. 035020.

[12] Liu, Tongqing, Hu, Lingling, and Han, Ming. "Adaptive ultrasonic sensor using a fiber ring laser with tandem fiber Bragg gratings." *Optics letters* Vol. 39 no 15 (2014), pp. 4462-4465.

[13] Han, Ming, Liu, Tongqing, Hu, Lingling, *et al.* "Intensity-demodulated fiber-ring laser sensor system for acoustic emission detection." *Optics express* Vol. 21 no 24 (2013), pp. 29269-29276.

[14] Zhao, Yang, Zhu, Yinian, Yuan, Maodan, *et al.* « A laser-based fiber Bragg grating ultrasonic sensing system for structural health monitoring." *IEEE Photonics Technology Letters* Vol. 28 no 22 (2016), pp. 2573-2576.

[15] Martinez, Christophe, Magne, Sylvain, and Ferdinand, Pierre. "Apodized fiber Bragg gratings manufactured with the phase plate process." *Applied optics* Vol. 41 no 9 (2002), pp. 1733-1740.

[16] Goossens, Sidney, Berghmans, Francis, and Geernaert, Thomas. "Spectral verification of the mechanisms behind FBG-based ultrasonic guided wave detection." *Sensors* Vol. 20 no 22 (2020), pp. 6571.

[17] Maurin, Laurent, Roussel, Nicolas, and Laffont, Guillaume. "Optimally temperature compensated FBG-based sensor dedicated to non-intrusive pipe internal pressure monitoring." *Frontiers in Sensors* Vol. 3 (2022). doi:10.3389/fsens.2022.835140

[18] Minardo, Aldo, Cusano, A., Bernini, Romeo, et al. "Fiber Bragg grating as ultrasonic wave sensors." In : Second European Workshop on Optical Fibre Sensors. SPIE, (2004). p. 84-87.